Progress In Electromagnetics Research, Vol. 112, 299–307, 2011

THE DESIGN AND FABRICATION OF A HIGHLY COMPACT MICROSTRIP DUAL-BAND BANDPASS FILTER

C.-Y. Chen and C.-C. Lin

Department of Electrical Engineering
National University of Tainan, Tainan, Taiwan, R.O.C.

Abstract—A highly miniaturized 2.45/5.7 GHz dual-band bandpass filter is presented in this paper. It shows that the proposed filter which combines different sizes of open-loop resonators can excite two desired passbands. With the meandered technology and fractal geometry, the overall size is extremely compact compared with the published dual-band bandpass filters. Furthermore, the skirt selectivity of the proposed filter with two transmission zeros locating at both sides of the passbands is much improved. The rejection of the spurious response from 6.7 GHz to 14.5 GHz is successfully suppressed to the level lower than −15 dB. The occupied area of the proposed filter is $9.8 \times 8.7\,\text{mm}^2$. The measurement is in good agreement with the simulation.

1. INTRODUCTION

A compact, low insertion and wide rejection band dual-band bandpass filter has come to be one of the recent trends in global system for mobile communications (GSM), wireless code-division multiple-access (WCDMA), and wireless local area networks (WLANs). Diverse techniques have been widely used and implemented in the design of the related dual-band bandpass filter. Surface-mountable planar dual-band bandpass filter with high performances are highly suitable for integration of the front-end of the RF transceiver in the wireless communication systems.

A dual-band bandpass filter using E-type resonators with compact size has been proposed [1]. Two resonant frequencies are excited by E-type resonators and short-circuited stubs. A single ring resonator with uniform and periodically stub-loaded configurations is applied

Received 13 November 2010, Accepted 13 January 2011, Scheduled 21 January 2011
Corresponding author: Chu-Yu Chen (cychen57@mail.nutn.edu.tw).

to design a compact dual-band filter with three transmission zeros between the two passbands [2]. In [3], stepped impedance resonators are commonly used in the dual-band filter designs. The component areas of the three architectures can be effectively reduced. And by appropriately selecting the impedance ratio and length ratio of the SIRs, the harmonic frequencies can be tuned for generating the dualbandpass response [4]. Besides, prototypes of microstrip lines loaded with C-MLSRR with and without series capacitive gaps are designed, which exhibit a negative permittivity behavior and a left-handed behavior, respectively, at the two operating frequencies [5]. In [6], dual-band bandpass filters with compact coupling and sizes reduction are proposed by using split ring steppedimpedance resonators and two paths coupling. Furthermore, the proposed dual-band filter with DGS technology [7] or stub loaded components [8] also has good dual-band performance. However, the skirt selectivity of each mentioned filter is required to be further improved for practical applications.

Fractal rules can be applied to miniature the RF component [9–15]. In this paper, the microstrip dual-band filter with fractal geometry is demonstrated. Incorporated with a 0° feed structure [16, 17], a fractal microstrip dual-band bandpass filter with high selectivity and miniaturized size is designed and fabricated.

2. DESIGN METHODOLOGY

The architecture of the proposed dual-band bandpass filter is shown in Fig. 1. Two transmission bands are excited and designed using proposed resonators which combine different size of open-loop resonators. The main resonators control the low-band resonant frequency and the sub resonators control the high-band resonant frequency. Fractal related geometry is founded to be very useful in reducing component size. Starting from the investigation of the

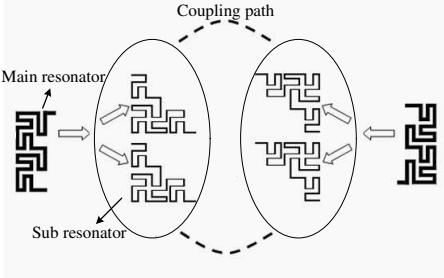

Figure 1. Architecture of the proposed dual-band bandpass filter.

behavior of radio waves, the phasor forms of the Maxwell's equations in a vacuum are represented as

$$\nabla \times \tilde{E} = -j\omega\mu\tilde{H}$$
$$\nabla \times \tilde{H} = j\omega\varepsilon\tilde{E}$$

where ε is the permittivity and μ the permeability of space. Observe that under the transformations $(\Delta x, \Delta y, \Delta z) \to (\lambda\Delta x, \lambda\Delta y, \lambda\Delta z)$ and $\omega \to \omega/\lambda$ for every scalar λ, the above equations are invariant. It is expected that the frequency is scaled by $1/\lambda$ when the wavelength is scaled by λ. Based on the above analysis, the fractal space-filling curves can be applied iteratively to reduce the sizes of the resonators. In this paper, the main resonators exciting the lower resonant frequency are meandered first and then the fractal sub resonators are embedded into the ends of the meandered main resonators to excite the higher resonant frequency. For a traditional open-loop half-wavelength resonator, each half-wavelength resonator exhibits maximum electric field density near the open ends of the resonator, and maximum magnetic field density around the center valley of the resonator during resonance. In the coupling structures, the electric and magnetic fringe field distributions at the coupled sides of two open-loop half-wavelength resonators produce electric and magnetic coupling, respectively. With careful design, both electric and magnetic couplings are capable of exciting the operation passbands in the RF filter design.

2.1. The Design of the Main Resonator

A half-wavelength resonator designed by hairpin shape was commonly used in the design of the RF filter. However, the large occupied area of the hairpin filter is a drawback in the filter design. To construct the highly miniaturized structure, the traditional hairpin structure shown in Fig. 2(a) is required to be meandered. The meandered type is shown in Fig. 2(b). Without changing the occupied area, the total length of

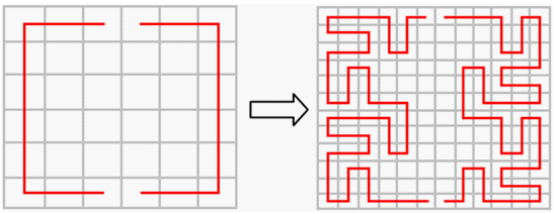

Figure 2. (a) The traditional hairpin structure. (b) The meandered hairpin structure.

the irregular shapes is increased to three times the length of the unmeandered type, which is equal to half-wavelength at the corresponding resonant frequency of $f_0/3$. Obviously, the modified geometry has proven to be 33% more efficient than the original structure.

2.2. The Design of the Sub Resonator

To embed the sub resonators into the meandered main resonators, fractal rules which can be used to miniaturize the resonator size are applied to redesign the sub resonators. To realize the fractal self-similarity property, a unit cell is firstly formed by meandering a conventional hairpin structure and then makes repetitive mapping. The fractal space-filling curves are iteratively constructed to reduce the component size. As shown in Figs. 3(a) and (b), the total length of the fractal structure using the first order fractal iteration can be increased about two times the length of the zero-th fractal iteration. The resonant frequency will be shifted to the lower band. The same occupied area based on the design of the resonant frequency of f_0 can be applied to design the resonant frequency of $f_0/2$ after using the first fractal iteration.

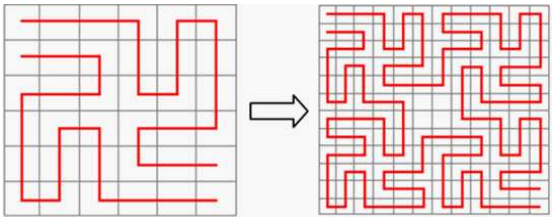

Figure 3. (a) Zero-th order fractal iteration. (b) First order fractal iteration.

When the width 2 mm is fixed, the length of the sub resonator in this design is 26.15 mm. The coupling effect resulted from the closely placed lines makes the effective length of the proposed filter become longer compared with the conventional one half wavelength resonator. However, the filter still can be designed into a small area without degrading the performance.

2.3. The Design of the Transmission Zeros

In [16, 17], the location of transmission zeros is investigated and calculated. In this paper, the feeding position must be placed at the proper position to separate the upper and lower path lengths based on

the assumptions of $\theta_2 = 1.3\theta_1$ and $\theta_1 + \theta_2 = 180°$. Here, θ_1 and θ_2 are the lower and upper path lengths, respectively. In the case of 5.7-GHz, the transmission zeros can be calculated by

$$f_1 = \frac{\frac{\pi}{2} f_0}{\pi - \theta_1}$$
$$f_2 = \frac{\frac{\pi}{2} f_0}{\theta_1}$$

And the upper and lower path lengths are selected as 9.61 mm and 7.39 mm corresponding to two transmission zeros $f_1 = 5.04$-GHz and $f_2 = 6.55$-GHz.

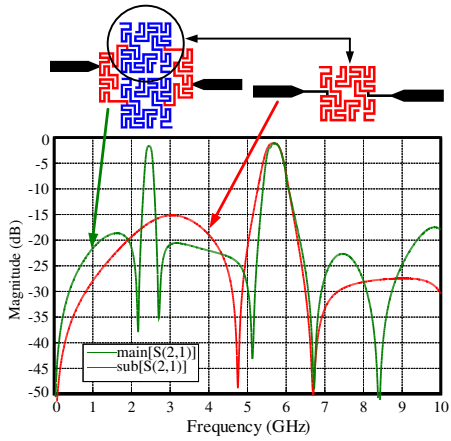

Figure 4. The simulation performances of the main and sub resonators.

As can be shown in Fig. 4, the sub resonator excites the resonant frequency at 5.7-GHz. Embedding the sub resonators into the main structure can produce both the frequencies of 2.45 and 5.7-GHz.

The possible radiation at the sharp corners is considered by the following EM simulation. In Fig. 5, it is shown that the simulation result of the filter with sharp corners is similar to the one with obtuse corners. They won't affect the performance very much at this operating frequency.

3. SIMULATION AND MEASUREMENT RESULTS

To demonstrate the applications of the studies in the previous sections, a fractal type compact dual-band bandpass filter operating at 2.45/5.7 GHz is proposed and implemented. The Zeland software IE3D is used to simulate the proposed structure. The main resonators and

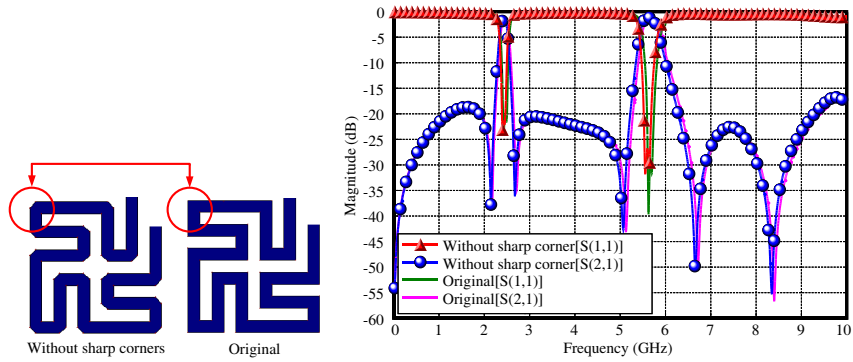

Figure 5. The simulation results of the original structure and the one with sharp corners.

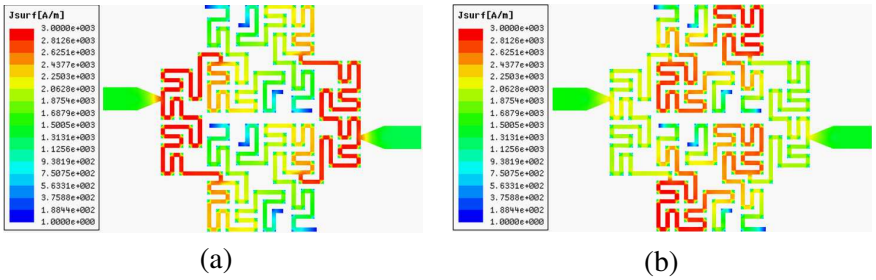

Figure 6. The electric current distribution. (a) 2.45 GHz. (b) 5.7 GHz.

the sub resonators are combined to construct a 2.45/5.7 GHz dual-band bandpass filter. As shown in Fig. 6, the coupling structures of the main and sub resonators are based on mixed coupling. The electric and magnetic fields at the coupled sides may have comparative distributions, so that both electric and the magnetic couplings occur. The proposed filter is designed and implemented on the RT/duroid 4003 substrate with a thickness $h = 20$ mil and a relative dielectric constant $\varepsilon_r = 3.38$. In Fig. 7, the dimensions of the proposed component are specified as the following parameters: $G_1 = 0.2$ mm, $G_2 = 0.45$ mm, $G_3 = 0.35$ mm, $G_4 = 0.25$ mm, $L_1 = 1.4$ mm, $L_2 = 1.1$ mm, $L_3 = 1.2$ mm, and $W_1 = 0.2$ mm. The occupied area of the proposed filter is $9.8 \times 8.7\,\text{mm}^2$. The measurement is in good agreement with the simulation. In Fig. 8, it shows the simulation and measurement results. The measurement insertion losses are lower than 2.47 dB at 2.4 GHz and 2.08 dB at 5.7 GHz. Besides, the return

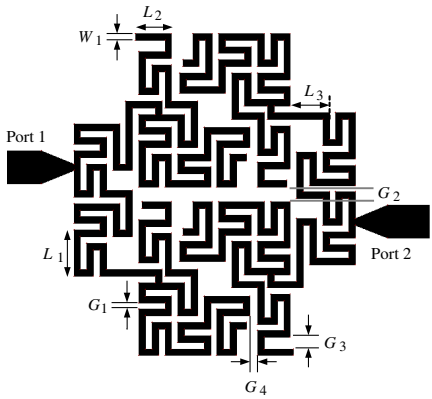

Figure 7. The dimension parameters of the proposed component.

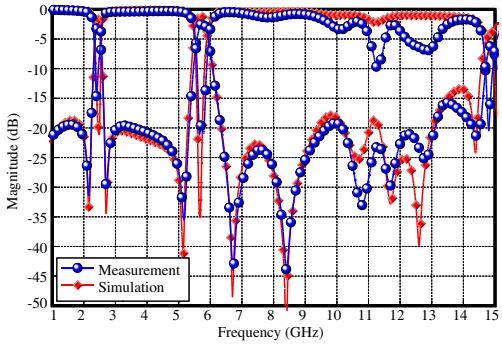

Figure 8. The measurement and simulation stopband performance.

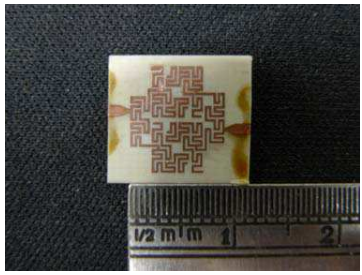

Figure 9. Photograph of the proposed filter.

losses are higher than 14.63 dB at 2.4 GHz and 20.56 dB at 5.7 GHz. In references [17], both 0° feed structure and non-0° feed structure are introduced and investigated. The skirt selectivity can be enhanced by creating transmission zeros in the 0° feed structure. In this paper, the dual 0° feed schemes are applied to produce two transmission zeros at the both sides of each passband. Compared with the traditional dual-band bandpass filters, the proposed filter shows not only good skirt selectivity, but also highly miniaturized size. Besides, the spurious response of the designed filter is considered to be effectively suppressed. The rejection of the spurious response from 6.7 GHz to 14.5 GHz is successfully suppressed to the level lower than −15 dB through the effect of mutual coupling. And the photograph of the proposed filter is shown in Fig. 9.

4. CONCLUSION

The ultimate goal in this paper is to design and fabricate the compact microstrip dual-band bandpass filter. For this purpose, the meandered technology and the fractal geometry are both utilized. Two transmission bands are excited and designed using proposed resonators which combine different size of open-loop resonators. The main resonators control the low-band resonant frequency and the sub resonators control the high-band resonant frequency. Also, the 0° feed structure applied to the two resonators can generate two transmission zeros which are 2.17/2.71 GHz and 5.13/6.6 GHz at both sides of the passbands. Compared with the published dual-band bandpass filters, an extremely compact microstrip dual-band bandpass filter is achieved. Furthermore, the skirt selectivity of the proposed filter with two transmission zeros locating at both sides of the passbands is much improved. Such a filter can be applied to the integration of products of IEEE 802.11g and IEEE 802.11a in wireless communication systems.

REFERENCES

1. Zhou, M., X, Tang, and F, Xiao, "Compact dual band bandpass filter using novel E-type resonators with controllable bandwidths," *IEEE Microw. Wireless Compon. Lett.*, Vol. 18, No. 12, 779–781, Dec. 2008.
2. Luo, S. and L. Zhu, "A novel dual-mode dual-band bandpass filter based on a single ring resonator," *IEEE Microw. Wireless Compon. Lett.*, Vol. 19, No. 8, 497–499, Aug. 2009.
3. Chu, Q.-X. and F.-C. Chen, "A compact dual-band bandpass filter using meandering stepped impedance resonators," *IEEE Microw. Wireless Compon. Lett.*, Vol. 18, No. 5, 320–322, May 2008.
4. Guo, L., Z.-Y. Yu, and L. Zhang, "Design of a dual-mode dual-band filter using stepped impedance resonators," *Progress In Electromagnetics Research Letters*, Vol. 14, 147–154, 2010.
5. Hu, X., Q. Zhang, and S. He, "Compact dual-band rejection filter based on complementary meander line split ring resonator," *Progress In Electromagnetics Research Letters*, Vol. 8, 181–190, 2009.
6. Xiao, J.-K. and H.-F. Huang, "New dual-band bandpass filter with compact sir structure," *Progress In Electromagnetics Research Letters*, Vol. 18, 125–134, 2010.
7. Wu, G.-L., W. Mu, X.-W. Dai, and Y.-C. Jiao, "Design of novel dual-band bandpass filter with microstrip meander-loop resonator

and CSRR DGS," *Progress In Electromagnetics Research*, Vol. 78, 17–24, 2008.

8. Velazquez-Ahumada, M. D. C., J. Martel-Villagr, F. Medina, and F. Mesa, "Application of stub loaded folded stepped impedance resonators to dual band filters," *Progress In Electromagnetics Research*, Vol. 102, 107–124, 2010.
9. Kim, I. K., N. Kingsley, M. Morton, R. Bairavasubramanian, J. Papapolymerou, M. M. Tentzeris, and J.-G. Yook, "Fractal-shaped microstrip coupled-line bandpass filters for suppression of second harmonic," *IEEE Trans. Microw. Theory Tech.*, Vol. 53, No. 9, 2943–2948, Sep. 2005.
10. Chen, W.-L., G.-M. Wang, and C.-X. Zhang, "Bandwidth enhancement of a microstrip-line-fed printed wide-slot antenna with a fractal-shaped slot," *IEEE Trans. Antennas Propag.*, Vol. 57, No. 7, Jul. 2009.
11. Ghosh, B., S. N. Sinha, and M. V. Kartikeyan, "Electromagnetic transmission through fractal apertures in infinite conducting screen," *Progress In Electromagnetics Research B*, Vol. 12, 105–138, 2009.
12. Zainud-Deen, S. H., H. A. El-Azem Malhat, and K. H. Awadalla, "Fractal antenna for passive UHF RFID applications," *Progress In Electromagnetics Research B*, Vol. 16, 209–228, 2009.
13. Camps-Raga, B. and N. E. Islam, "Optimized simulation algorithms for fractal generation and analysis," *Progress In Electromagnetics Research M*, Vol. 11, 225–240, 2010.
14. Yu, Z.-W., G.-M. Wang, X.-J. Gao, and K. Lu, "A novel small-size single patch microstrip antenna based on Koch and Sierpinski fractal-shapes," *Progress In Electromagnetics Research Letters*, Vol. 17, 95–103, 2010.
15. Patin, J. M., N. R. Labadie, and S. K. Sharma, "Investigations on an H-fractal wideband microstrip filter with multi-passbands and a tuned notch band," *Progress In Electromagnetics Research B*, Vol. 22, 285–303, 2010.
16. Tsai, C.-M., S.-Y. Lee, and C.-C. Tsai, "Hairpin filters with tunable transmission zeros," *IEEE MTT-S Int. Microw. Symp. Dig.*, Vol. 3, 2175–2178, 2001.
17. Tsai, C.-M., S.-Y. Lee, and C.-C. Tsai, "Performance of a planar filter using a 0° feed structure," *IEEE Trans. Microw. Theory Tech.*, Vol. 50, No. 10, 2362–2367, Oct. 2002.